# X-RAY DIFFRACTION STUDIES OF HIGH-PURITY IRON: TOPOGRAPHY AND DOUBLE-CRYSTAL DIFFRACTION

Tsukuda, Noboru
Research Institute for Applied Mechanics, Kyushu University : Research Associate

Kitajima, Kazunori
Research Institute for Applied Mechanics, Kyushu University : Professor

https://doi.org/10.5109/6617895

出版情報：Reports of Research Institute for Applied Mechanics. 26 (81), pp.83-97, 1978-07. 九州大学応用力学研究所
バージョン：
権利関係：

Reports of Research Institute for Applied Mechanics
Vol. XXVI, No. 81, 1978

# X-RAY DIFFRACTION STUDIES OF HIGH-PURITY IRON: TOPOGRAPHY AND DOUBLE-CRYSTAL DIFFRACTION

By Noboru TSUKUDA* and Kazunori KITAJIMA**

High-purity iron single crystals with low dislocation density were prepared and examined by X-ray topography and X-ray double-crystal diffraction. Transmission X-ray topographs showed isolated dislocations, dislocations lying along subgrain boundaries and magnetic domain walls.

Single crystals of silicon and gadorinium gallium garnet (GGG) are also examined with a single-crystal arrangement and a moderate-and a high-angle double-crystal arrangement. For measurements of lattice parameter change above liquid nitrogen temperature, a metal cryostat for X-ray diffraction were made. Experimental results of the lattice parameter change and the thermal expansion coefficient of iron are in good agreement with those of other works.

## 1. Introduction

X-ray diffractin techniques has often been employed for investigations of imperfections in solids. Such imperfections as self-interstitials, vacancies, dislocations and impurities give rise to dilatation and distortion of the lattice, which can be known by measurements of lattice parameter change and X-ray diffuse scattering, respectively.

Studies on self-interstitials in metals have been developed in recent years by many researchers. Knowledge of structures and annealing behaviour of interstitials may evidence the dispution between the one-interstitial model and the two-interstitial model.[1] There has been a long lying question on the interpretation of annealing stage I and III. The two-interstitial model proposed by Seeger and his co-workers (Stuttgart group) is that stage I has been resulted from migration of interstitial crowdions and free interstitials just begin to migrate at stage III. On the other hand, the one-interstitial model proposed by Jülich group is that free interstitials migrate at stage I and stage III is caused by migration of vacancies. Detailed defect structures has been investigated in very recent years by use of X-ray diffraction

* Research Associate, Research Institute for Applied Mechanics, Kyushu University.
** Professor, Research Institute for Applied Mechanics, Kyushu University.

techniques mainly lattice parameter change and diffuse scattering.[2),3)]

Lattice parameter change $\Delta a/a$ and diffuse scattering (Huang scattering) $I_H$ caused by point defects and their clusters are represented as follows:

$$\Delta a/a=-\frac{1}{3}c_i Tr P_{ij}/V_c(c_{11}+2c_{12}) \tag{1}$$

$$I_H=c_i f_h^2|\boldsymbol{h}\cdot\boldsymbol{t}(\boldsymbol{q})|^2 \tag{2}$$

where $c_i$ is the concentration of point defects, $V_c$ the atomic volume, $\frac{1}{3}(c_{11}+2c_{12})$ the bulk modulus, $P_{ij}$ the element of the elastic dipole tensor (double force tensor), $f$ the atomic scattering factor and $\boldsymbol{t}(\boldsymbol{q})$ the Fourier transform of the displacement field. $P_{ij}$, which is analoguous to electric dipole tensor in an electric field, and $\boldsymbol{t}(\boldsymbol{q})$ are in the relation:

$$\boldsymbol{t}_i(\boldsymbol{r})=\sum_{j,l}\frac{\partial}{\partial \boldsymbol{x}_l}\boldsymbol{r}_l G_{ij}(\boldsymbol{r})P_{jl}, \tag{3}$$

where $\boldsymbol{t}_i(\boldsymbol{r})$ is the asymptotic displacement, $G_{ij}(\boldsymbol{r})$ the Green function. When the defects have cubic symmetry in the crystal, Eq. (2) is rewritten by use of Eq. (3) for (h k 0) refiections with [1 0 0] and [1 1 0] directions.

$$I_H=c_i f_h^2\left(\frac{\boldsymbol{h}}{\boldsymbol{q}}\right)^2 Tr P_{ij}/3V_c^2, \tag{4}$$

while $\gamma^{(1)}$ is a quantity depending on elastic constants and reciprocal lattice vector $\boldsymbol{h}$ and $\boldsymbol{q}$. The volume change by a point defect $\Delta V_{rel}$ is directly caluculated as

$$\Delta V_{rel}=Tr P_{ij}/(c_{11}+2c_{12}). \tag{5}$$

Both measurements of $\Delta a/a$ and $I_H$ can determine $c_i$, $Tr P_{ij}$ and $\Delta V_{rel}$. Recent researchers determined for Cu[10),11),12)], Al[13)], Au[14)] and Mo[15)] and revealed fundamental characteristics and thermal activation processes.

Intensity measurements of the Huang scattering, however, has to get over various difficulties. Thermal diffuse scattering or Compton scattering obstruct the Huang scattering above very low temperature.[16)] Moreover, larger dislocation density may broarden the rocking curve and may cover the Huang scattering. Goniometers and detectors for this purpose are also required high angular resolution and accurate counting of the diffracted beam, respectively. Lattice parameter change by radiation-induced defects in metals is the order of $10^{-5}\sim10^{-4}$, which is corresponds the change of Bragg angle of $10^{-3}\sim10^{-2}$ degree in arc. The graduation of usual diffractometers are $10^{-2}$ degree in arc and are unsatisfactory for this measurements. In our present experiments of iron, (8 0 0) reflection with Mo $K\alpha_1$ radiation were measured. Relative lattice parameter change, $\Delta a/a$, of $1\times10^{-5}$ corresponds 14 sec of arc at room temperature. So that a high-precision goniometer (Kohzu-Seiki KTG-11S) was utilized.

## 2. Preperation of Samples

Original sample materials (Materials Research Corporation MARZ Grade) were zone-refined in wet hydrogen (1 pass) and dry hydrogen (6 passes). Further purification was performed by electron-beam floating zone melting technique in vacuo ($1.2\times10^{-6}$ mmHg). The residual resistance ratio ($\rho_{R.T}/\rho_{4.2K}$) of this purified material is about 2000.

The purified material (5 mm in diameter) was cross-rolled and cut to square slices ($10\times10\times0.4$ mm). The secondary recrystallization method was attempted to obtain single crystals. Stored energy introduced by cold-working is released by high temperature annealing and is to the driving force of the growth of recrystallized region (primary recrystallization). Some of these recrystallized regions containing low density of dislocations and being stress-free begin to start further growth of recrystallized region (secondary recrystallization). The driving force of this recrystallization is the surface energy of grain boundaries. Sliced materials were annealed at 880°C in wet hydrogen for 14 hours, then gradually cooled at rate of 100°C/h. Further annealing at 650°C in dry hydrogen was performed for 12 hours. The surfaces of the single crystals (dimension 30~100 mm$^2$) are parallel to (1 0 0) plane.

## 3. Topography

Topography are advantageous for following investigations: three-dimensional arrangement of low-angle boundaries and dislocations; determination of the Burgers vector; ferromagnetic domain structures. It seems to be rather small number of X-ray transmission topographic studies on pure iron[17),18)]. It may be caused by the difficulties of preperation of large single crystals containing low-density dislocations. Dislocation density of $10^{-6}$/cm$^2$ or less is required for transmission topographs. Higher purity realizes lower density of dislocations[19)]. Ferromagnetism also complicates the topographic study of iron. Above mentioned defects bring on displacement field which causes the contrast of topographs. Dynamical theory of X-ray diffraction for slightly distorted crystals explains the contrast[20),21)].

A function $f(x, z)$, presenting effects of distortions is described as

$$f(x, z)=\pi\left(\frac{\partial^2}{\partial z^2}-c^2\frac{\partial^2}{\partial x^2}\right)(\boldsymbol{g}\cdot\boldsymbol{u}) \tag{6}$$

where $\boldsymbol{g}$ is the reciprocal lattice vector of the diffraction and $\boldsymbol{u}(\boldsymbol{r})$ the displacement vector at position $\boldsymbol{r}$. The first term in the light hand side represents the geometrical bending effect of the lattice, while the second term the differential of the change of the lattice spacing. The sign of $f(x, z)$ characterizes the contrast around the distortions for each condition of absorption effects as follows:

| $\mu_0 t$ | $f$ | contrast |
|---|---|---|
| $<1$ | $\gtrless 0$ | black |
| $2\sim3$ | $>0$ | black |
| | $<0$ | white |
| $>10$ | $\gtrless 0$ | white, |

where $\mu_0$ and $t$ are the mass absorption coefficient and the thickness of the crystal, respectively. Because of the rather large region of $\mu_0 t$, more complicated contrasts in the topographs were observed. Fig. 1 shows a schematic drawing of the dittraction geometry of our experiment. As for their ferromagnetisn, internal 90° Bloch walls also give rise to a variety of the X-ray diffraction contrasts which under certain conditions are comparable in strength with those from the dislocations[22], 180° walls, however, produce no diffraction contrast.

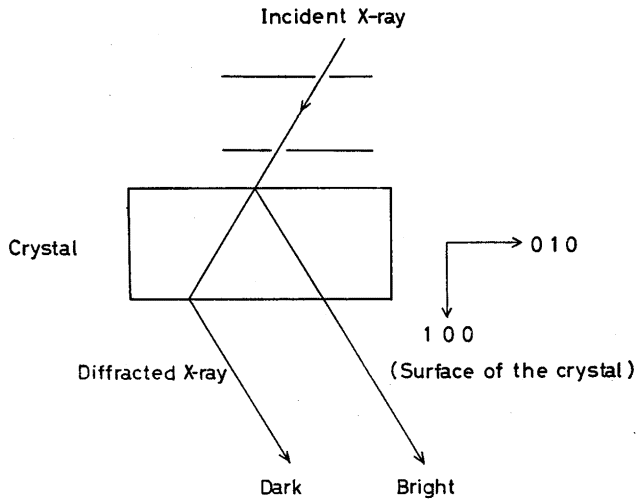


Fig. 1. Schmatic drawing of the diffraction geometry of the transmission topographs. Dark, Borrmann topograph: Bright, Lang topograph.

Specimens for the topographic studies were prepared from a single crys tal of iron, detailed at the preceding section, by chemical thinning and further annealing. A single crystal about 15 mm$^2$ in area and 0.4 mm thick were thinned to 0.1$\sim$0.2 mm in a solution of 95cc $H_2O_2$+5cc HF. For removement of the strain which may be introduced by handling or thinning,

further annealing was performed in wet hydrogen atmosphere for 6 hours then gradually cooled.

Transmission topographs were obtained for some reflections; (0 2 0), (0 1 1), (1 1 0) and (1 $\bar{1}$ 0). Mo $K\alpha$ radiation was used on the condition 55 KV and 8 mA. Because of large absorption effect ($\mu t = 3 \sim 5$), rather large exposure time was needed (about 10 hours). Ilford nuclear emulsions were used for X-ray recordings.

The absorption effect for (1 1 0) and (1 $\bar{1}$ 0) reflections are larger than that of (0 2 0) and (0 1 1) reflections. Fig. 2(a) shows a topograph of (0 2 0) reflection, in which the Bloch walls (straight lines along 0 1 1 and

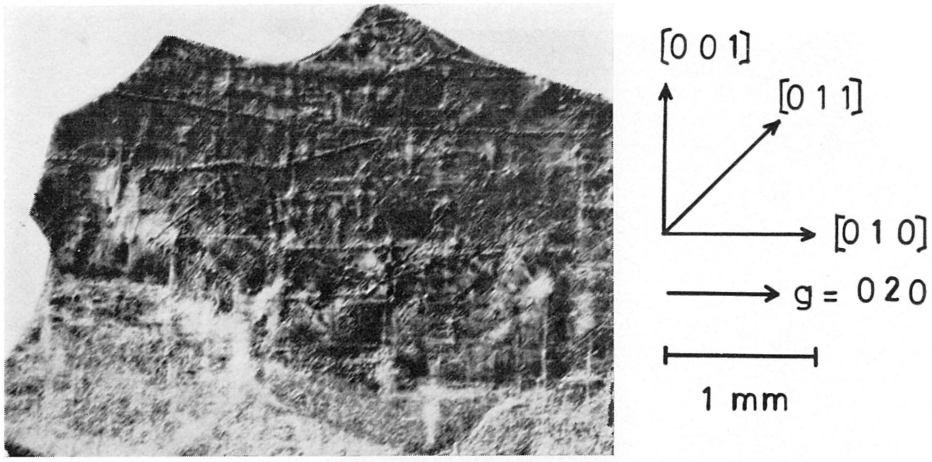


Fig. 2(a) Topograph of 020 reflection. g: the reciprocal lattice vector of the diffraction.

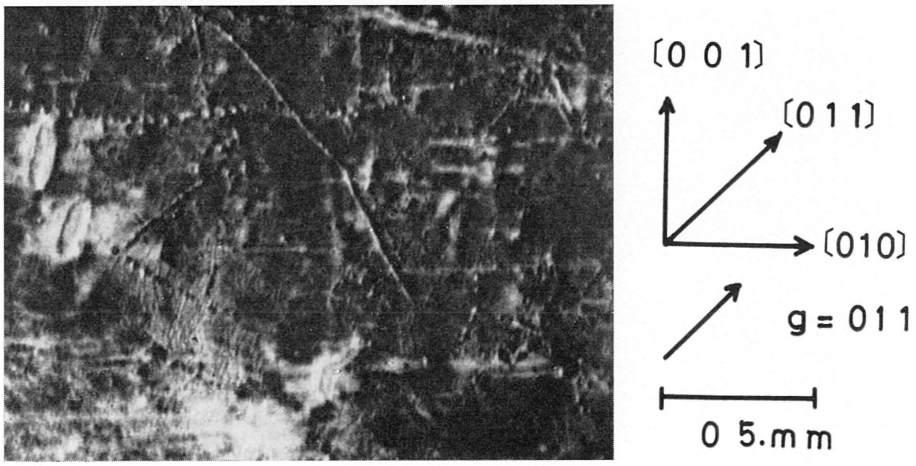


Fig. 2(b) Topograph of 011 reflection. $g = 011$

0 1 $\bar{1}$ directions), and dislocations are observed. The contrast of the dislocations is conspicious at the Bloch walls and is somewhat a black and white image. Rather larger density of dislocations is observed at underside of Fig. 2(a). Fig. 2(b) shows a (0 1 1) topograph of the crystal rotated 45° around [1 0 0]. The contrast of the Bloch walls along [0 1 $\bar{1}$] becomes to vanish because of the invissible condition $\boldsymbol{g}\cdot(\boldsymbol{m}_1-\boldsymbol{m}_2)=0$, where $\boldsymbol{m}_1$ and $\boldsymbol{m}_2$ are the vectors parallel to the easy directions of magnetization on the both sides of the walls. An array of dislocations is observed along the subgrain boundary, which is also confirmed with an observation of etch-pit. Fig. 2(c) shows a (1 1 0) topograph. A reverse contrast of upper-and lower-side is

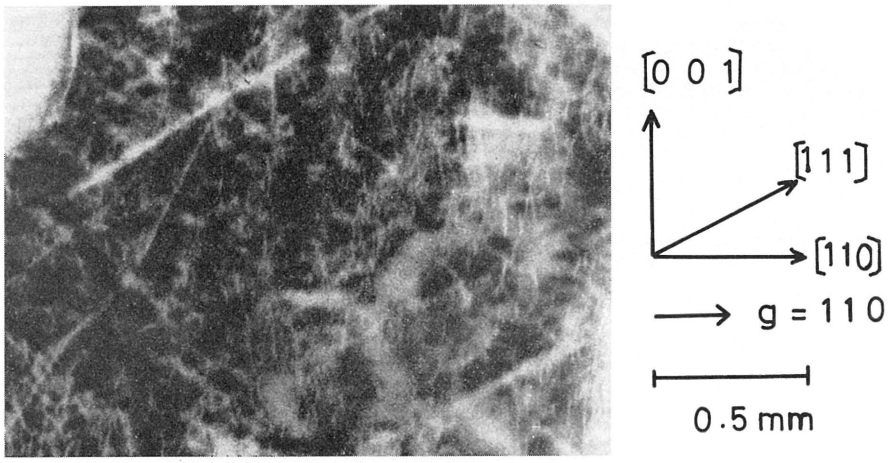


Fig. 2(c) Topograph of 110 reflection. $g=110$

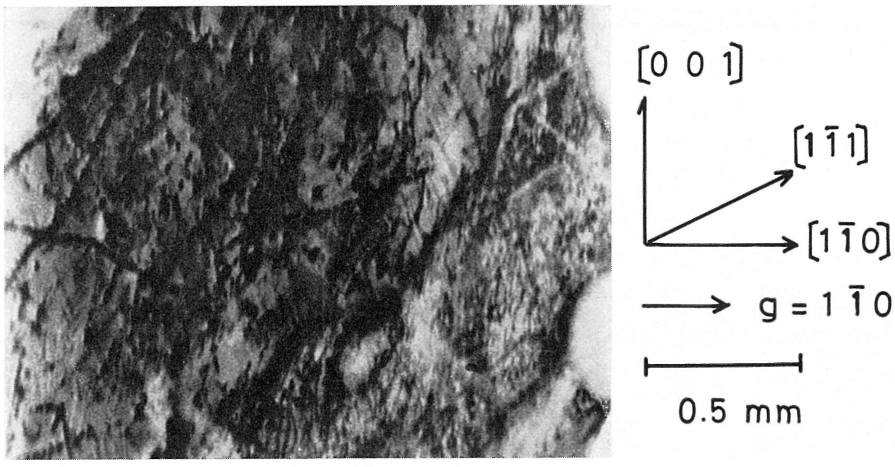


Fig. 2(d) Topograph of $1\bar{1}0$ reflection. $g=1\bar{1}0$

observed. These complicated images are the consequence of large $\mu_0 t$, as mentioned above. Fig. 2(d) shows a (1 $\bar{1}$ 0) topograph. The contrast of upper-side reverses with that of (1 1 0) topograph. Dislocations in this topograph are clear white lines. This is the particular to the Borrmann topographs.

## 4. Double-Crystal diffraction

### 4.1 Setup for X-ray measurements

Lattice parameter measurements by X-ray diffraction have long been practiced. The relative error $\Delta a/a$ is estimated from differential form of the Bragg low $2d\sin\theta=\lambda$:

$$d/d=\Delta\lambda/\lambda-\cot\theta\Delta\theta \qquad (7)$$

The natural width of the characteristic radiation spectra $\Delta\lambda/\lambda$ are the order of $10^{-4}$. The Precision with the single-crystal or dispersive double-crystal diffraction arrangements may be therefore, less than the order of $10^{-5}$. Wavelength-dispersion, however, can be eliminated with a parallel double-crystal diffraction arrangement. The second term in the right-hand side of Eq. (7) is the spread or change of the diffracted X-ray, and is superposed

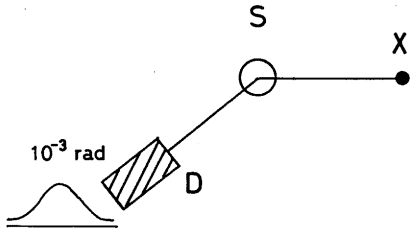


Fig. 3(a) Schematic drawing of single-crystal diffraction arrangement.

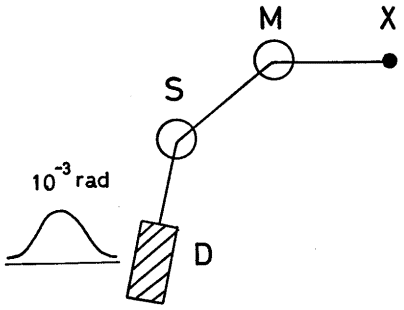


Fig. 3(b) Dispersive double-crystal diffraction arrangement.

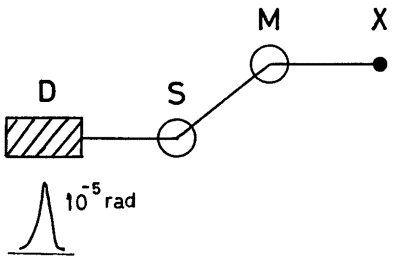


Fig. 3(c) non-dispersive (parallel) double-crystal diffraction arrangement.

with some causes, i.e. the geometrical divergence of the incident and the diffracted X-ray and originated from measureing system. Figs. 3(a), 3(b) and 3(c) show the single-crystal, dispersive double-crystal and parallel double-crystal diffraction arrangements, respectively.

Lattice parameter measurements with high-angle double-crystal diffraction technique have well been practiced by A. Okazaki and his co-workers[23),24)]. The advantage of this technique is mentioned below: (i) high-sensitivity of $\theta$, and (ii) high-accuracy of $\theta$. When a lattice parameter change is identical, the larger Bragg angle (smaller value of $\cot\theta$) brings larger change of $\theta$.

In the first place, we have examined geometrical conditions such as incident slits. The contribution of the vertical divergence of incident X-ray to the width of the rocking curve is estimated as $\frac{1}{2}\phi^2\tan\theta$, where $\phi$ is the spread of X-ray along vertical direction and $\tan\theta$ is 6.9 for (8 0 0) reflection with Mo K. The vertical divergence with a slit being 10 mm in vertical length is sufficiently small than that of horizontal direction.

Next, by single-crystal diffraction arrangement, iron, silicon (dislocation free) and GGG are examined as the nature of the monochromator crystals. Table 1 shows larger FWHM (Full-Width at Half-Maxmum) and the intensity of the iron than that of GGG. It seems to larger area of the iron crystal. The dependence of FWHM of reflecting curve on resolution parameter $\tan\theta/\tan\theta_M$ is discussed by Willis that the reflecting curve is a minimum in the region of $\theta=\theta_M$, where $\theta_M$ is Bragg angle of a monochromator crystal.

Table 1.

| Specimen | Reflection | Bragg Angle (deg) | FWHM (sec) |
|---|---|---|---|
| Iron (MRC) | 2 0 0 | 28.65 | 50 |
| | 8 0 0 | 81.77 | 350 |
| Silicon | 1 1 1 | 6.50 | 50 |
| | 4 4 4 | 26.90 | 100 |
| GGG | 20 20 20 | 82.81 | 250 |

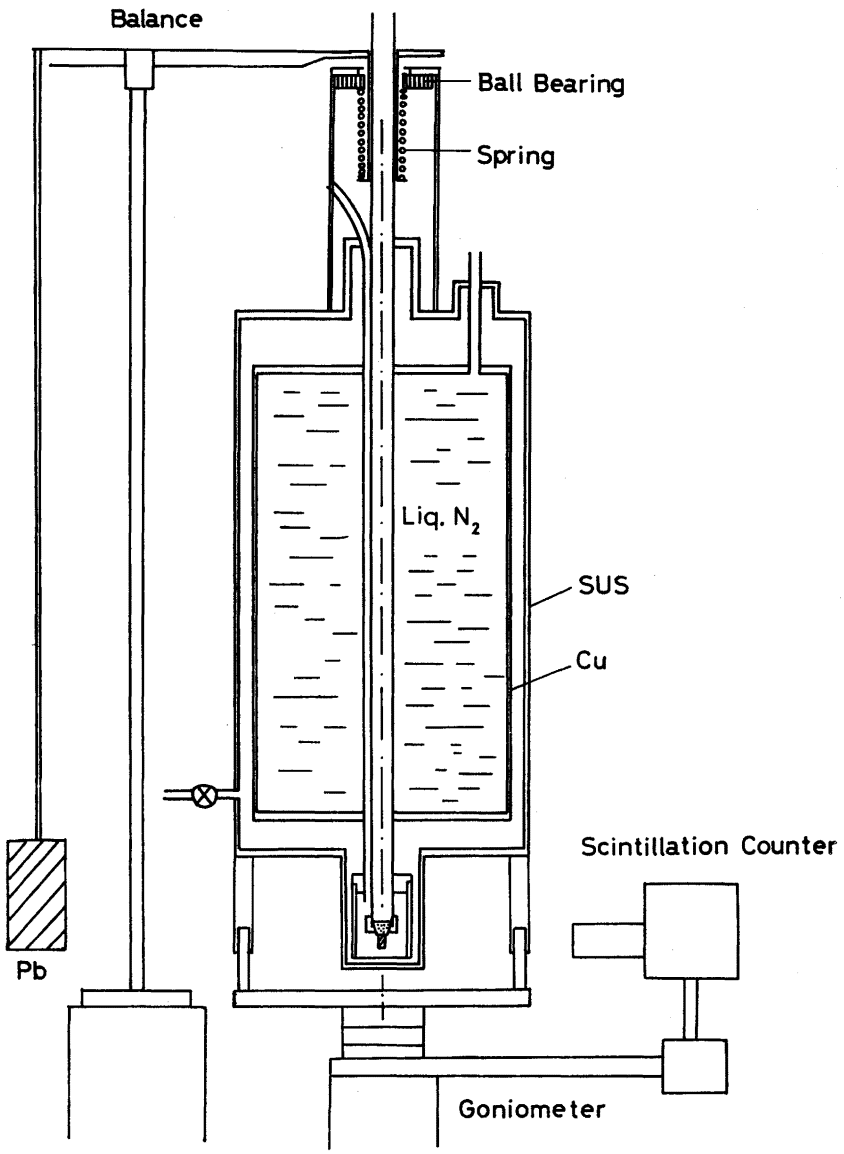


Fig. 4 Liguid nitrogen cryostat for X-ray diffraction. The goniometer is rotated by a pulse-motor.

The goniometer for the monochromator crystal was made in our laboratory. A motion of the micrometer with 1/100 mm corresponds to the rotation of the monochromator crystal with 10 sec of arc. The precision of the goniometer is sufficient for the present measurement. For specimen crystal, a high precisoin goniometer is made to use. The angular precision is 0.1 sec of arc and the crystal can be rotated within 7 degree of arc.

### 4.2 Cryostat for X-ray diffraction

By use of a metal cryostat, lattice parameter measurements on iron single crystals between 77 K and 300 K were performed. A specimen can be mounted without temperature increasing above 77 K and without breaking vacume of the cryostat. These specialities are indispensable for the measurements of irradiated specimens[25]. The weight of this cryostat is about 13 kg with liqurd nitrogen. So, it is too heavy for mounting on the goniometer, that we hung it with a balance. A shematical drawing of the cryostat is shown in Fig. 4. Capacity and evaporation rate of liquid nitrogen are 4000 cc and 150 cc/h, respectively. Then, no further transfer is needed during usual measurements. The specimen chamber made of copper blocks is coated by Aluminum thin films and its window is made from 0.05 mm thick Mylor films also coated with evaporated Aluminum. A specimen holder equipped with a heating device is shown in Fig. 5. The holder (70 cm in length) is inserted to the specimen chamber through stainless steel guide tube and fixed with tapered part. The heating device, back to back with a specimen, is of 0.1 mm$\phi$ manganin wires (120 $\Omega$). Liquid nitrogen in the speci-

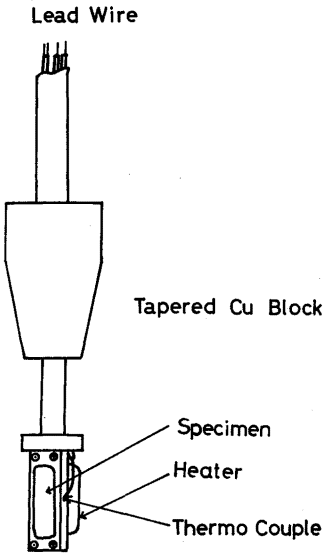


Fig. 5 Specimen holder and heating device.

men chamber is evaporated out by heating and measurements are carried out in the nitrogen gas atmosphere. Temperature of a monochromator, as well as a specimen crystal, is in need of controlling. Two kinds of controlling equipments are in use. One is PID SCR controller for monochromator and the other is a controller in which a light-coupled transistor (TLP 503) is incorporated in the amplifier circuit[26].

The temperature of the monochromator crystal is kept $300\pm0.02$ K during measurements, while that of the specimen crystal is controlled at any temperature whthin $\pm0.1$ K above 82 K.

### 4.3 Use in Double-Crystal Diffraction

Single crystals of iron and silicon were examined with various double-crystal diffraction arrangements. The FWHM and the intensities are listed in Table 2. The letters denote the kinds of these arrangements; H: high

Table 2.

| Specimen | Reflection | Arrangement | FWHM (sec) |
|---|---|---|---|
| Iron | | | |
| (MRC) | 2 0 0 | M, D | 170 |
| | 2 0 0 | M, P | 16 |
| | 8 0 0 | H, P | 70 |
| (Electl) | 8 0 0 | H, P | 600 |
| Silicon | 4 4 4 | M, D | 100 |
| | 4 4 4 | M, P | 14 |

angle, M: moderate angle, D: wavelength-dispersive (+, +), P:parallel (+, −). Molybdenum K radiation was used on the condition 55 kV and 160 mA. The FWHM of a dispersive arrangement is 10 times larger than that of parallel arrangement for both cases (angular ranges and materials). Larger values of the FWHM of rocking curves of high-angle diffraction is understood from Eq. (7) by

$$\Delta\theta=\left(\frac{\Delta\lambda}{\lambda}-\frac{\Delta d}{d}\right)\tan\theta. \tag{8}$$

Eq. (8) shows the tangent dependence of the FWHM on the scattering angle. The FWHM of MRC iron is as same as that of silicon but that of electrithic iron. This means that single crystals of MRC iron are with high-perfection (low dislocation density), while that of electrithic iron are consist of mosaic crystals. Change of the Bragg angle of 4 sec of arc can be detected for a (8 0 0) reflection and is corresponds $2\times10^{-6}$ of $\Delta a/a$.

Relative lattice-parameter change and thethermal expansion coefficient of iron are shown in Fig. 7. They are in good agreement with those of other works[27].

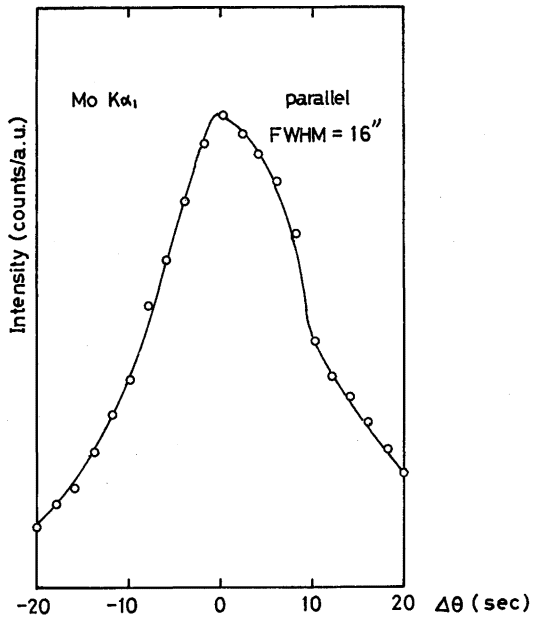


Fig. 6. Rocking curve of 200 reflection of high-purity iron.

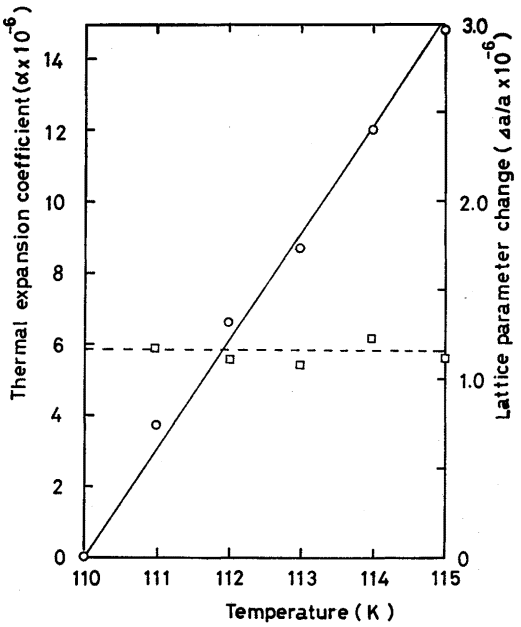


Fig. 7. Relative lattice parameter change (○) and thermal expansion coefficient (□) of iron.

## 5. Discussion

Investigation of interstitials in metals can be performed with realization of the conditions below: i) low temperature irradiation ii) preperation of single crystals with high-purity and low dislocation density iii) cryostat for X-ray diffraction iv) precise measurements.

i) The irradiation were performed by use of linear accelerator (LINAC) at Kyoto University reactor laboratory (KUR). Specimens were irradiated in the stream of liquid nitrogen. Details of the irradiation experiment are reported elsewhere[28].

ii) As described in section 2, it is not so easy to prepare single crystals of high-purity iron with low dislocation density. This may be one of the reason why not so large investigations of interstitials in iron by X-ray diffraction technique have been performed.

iii) A cryostat for the investigation of interstitials in metals is particular. That is, specimens has to be transfered and mounted on the cryostat without temperature increasing, which let the interstitials begin to migrate.

iv) The measurements of lattice parameters on irradiated metals have been performed mainly by two methods. One is the rotating single-crystal back reflection technique with monochromatic radiation (fine-focus tube)[2]. The resolution of $\Delta a/a$ is $6.5\times10^{-6}$. and is limited by the dispersed profiles of single spectral lines. The other technique, is employed by Larson[29], is by mutiple Bragg reflection geometry. This technique was first succeeded by Hart[30]. In this case, changes of Bragg angle are measured in a non-dispersive double-crystal arrangement. This method, however, is not common, because two X-ray source or a monolithic monochromator crystal (same substance with the specimen) are required.

Non-dispersive high-angle double-crystal diffraction can be easily used similar to a common single-crystal diffraction. Precision of $\Delta a/a$ depends only the intrinsic profile of the crystal and is $2\times10^{-6}$ for our experiment. This is sufficient for present study. This technique can widely be used for other studies.

### Acknowledgements

The authors are grateful to Prof. A. Okazaki, Dr. N. Ohama and Mr. H. Sakashita for helpful discussions, to Mr. T. Fujiwara for aid of the experiment. They also want to thank Prof. K. Futagami and Mr. Y. Akashi for facilities for the use of the X-ray generator. This work was partially supported by the Grant-in Aid for Scientific Research from the Ministry of Education.

**References**


1) Seeger, A.: *Introduction to the panel discussion, Vacancies and Interstitials in Metals*, ed. Seeger, A. et al, North Holland, Amsterdam (1970) pp. 999.
2) Wagner, H., Dworschak, F. and Schilling, W.: *Comparison of Lattice-Parameter and Resistivity Change in Electron-Irradiated Aluminum*, Phys. Rev. B **2** (1970) pp. 3856.
3) Ehrhart, P., Haubold, H.-G. and Schlling, W.: *Investigation of Point Defects and Their Agglomerates in Irradiated Metals by Diffuse X-Ray Scattering*, Adv. Solid State Phys. **14** (1974) pp. 87.
4) Kanzaki, H.: *Point Defects in Face-Centered Cubic Lattice I Distortion around Defects*, J. Phys. Chem. Solids. **2** (1957) pp. 24.
5) Huang, K.: *X-Ray Reflections from Dilute Solid Solutions*, Proc. Roy. Soc. A **190** (1947) pp. 102.
6) Dederichs: *The Theory of Diffuse X-Ray Scattering and its Application of Point Defects and Their Clusters*, J. Phys. F: Metal Phys. **3** (1973) pp. 471.
7) Trinkaus, H.: *On Determination of the Double-Force Tensor of Point Defects in Cubic Crystals by Diffuse Scattering*, phys. stat. sol. (b) **51** (1972) pp. 307.
8) Trinkaus, H.: *On the Investigation of Small Dislocation Loops in Cucic Crystals by Diffuse X-Ray Scattering*, phys. stat. sol. (b) **54** (1972) pp. 209.
9) Peisl, H.: *Diffuse X-Ray Scattering from the Displacement Field of Point Defects and Defect Clusters*, J. Appl. Cryst. **8** (1975) pp. 143.
10) Ehrhart, P. and Schlagheck, U.: *Investigation of Frenkel Defects in Electron Irradiated Copper by Huang Scattering of X-Rays I*, J. Phys. F: Metal Phys., **4** (1974) pp. 1575.
11) Ehrhart, P. and Schlagheck, U.: *Investigation of Frenkel Defects in Electron Irradiated Copper by Huang Scattering of X-Rays II*, J. Phys. F: Metal Phys., **4** (1974) pp. 1589.
12) Larson, B.C. and Young, Jr, F.W.: *A Cmparison of Diffuse Scattering by Defects Measured in Anomalous Transmission and Near Bragg Reflections*, Z.. Naturforsch **28 a** (1973) pp. 626.
13) Ehrhart, P. and Schlling, W.: *Investigation of Interstitials in Electron-Irradiated Aluminum by Diffuse X-Ray Scattering Experiments*, Phys. Rev. B **8** (1973) pp. 2604.
14) Ehrhart, P. and Segura, E.: *X-Ray Investigation of Interstitials and Interstitial Clusters after Low Temperature Irradiation and Thermal Annealing of Gold*, Proc. Int. Conf. on Fundamental Aspects of Radiation Damage in Metals, Vol. **1**, pp. 295. Gatlinburg Tenn. U.S.A. (1975).
15) Ehrhart, P.: *Interstitials and Interstitial Clusters in BCC and HCP Metals Investigated by Huang Diffuse Scattering*, ibid. pp. 302.
16) Haubold, H.-G.: *Measurement of X-Ray Scattering between Reciprocal Lattice Points as a New Experimental Method in Determining Interstitial Structures*, J. Appl. Cryst. **8** (1975) pp. 175.
17) Yamashita, T. and Mihara, A.: *Magnetic Domain Walls in Zone Melted Metal Iron Crystals as Observed by X-Ray Diffraction Topography*, Japan. J. Appl. Phys. **10** (1971) pp. 1661.
18) Futagami, K. *Parallel Dislocation Images on the X-Ray Diffraction Topograph in Iron Single Crysals*, Japan. J. Appl. Phys. **11** (1972) pp. 814.
19) Kadečková, S. and Šesták, B.: *Dislocation Structure in "As-Grown" High-Purtity*

*Iron Single Crystals*, Can. J. Phys. **45** (1967) pp. 1041.
20) Ando, Y. and Kato, N.: *X-ray Diffraction Phenomena in Elastically Distorted Crystals*, J. Appl. Cryst. **3** (1970) pp. 74.
21) Azároff, L. V., Kaplow, R., Kato, N., Weiss, R. J., Wilson, A. J. C. and Young, R. A.: *X-Ray Diffraction*, WcGraw-Hill, New York, (1974).
22) Lang, A. R. and Polcarová, M.: *X-ray Topographic Studies of Dislocations in Iron-Silicon Alloy Single Crystals*, Proc. Roy. Soc. A **285** (1965) pp. 297.
23) Okazaki, A. and Kawaminami, M: *Accurate Measurement of Lattice Constants in a Wide Range of Temperature: Use of White X-Rays and Double-Crystal Diffractometry*, Japan, J. Appl. Phys. **12** (1973) pp. 783.
24) Kaneda, T, Kawaminami, M, Ohama, N, Okazaki, A. and Sakashita, H: *X-Ray Monochromators for High-Angle Double-Crystal Diffraction*, Japan. J. Appl. Phys. **16** (1977) pp. 623.
25) Maeta, H, Kato, T. and Okuda, S.: *A Low-Temperature Cryostat for X-ray Diffraction Work*, J. Appl. Cryst. **9** (1976) pp. 378.
26) Matsuo, T.: *Construction of a Light-Coupled Power Amplifier for Use in a Temperature-Controller*, NETSUSOKUTEI **4** (1977) pp. 54, (in Japanese).
27) Corruccini, R. J. and Gniewek, J. J.: *Thermal Expansion of Technical Solids at Low Temperatures*, Natn. Bur. Stand. Monograph **29** (1961) U. S. Govt. Printing Office, Washington, D. C..
28) Kitajima, K., Futagami, K., Kuramoto, E., Abe, H., Tsukuda, N., Akathi, Y., Yoshida, H. and Fujita, Y.: *Application of KUR LINAC to the Study of Radiation Damage of Metals*, Ann. Rep. Reactor Inst., Kyoto Univ. **10** (1977).
29) Larson, B. C.: *High-Precision Measurements of Lattice Parameter Changes in Neutron-Irradiated Copper*, J. Appl. Phys. **45** (1974) pp. 514.
30) Hart, M.: *High-Precicion Lattice Parameter Measurements by Multiple Bragg Reflection Diffractometry*, Proc. Roy. Soc. A. **30** (1969) pp. 281.

(Received May 8, 1978)